A Waveform Design Method of Dense False Target Jamming Suppression

Leilei Xu[1], Jun Pan[1], Juqi Yin[1, a1], Yutai Zhou[1], Hao Meng[1], Sheng Zheng[1], Yulong Wei[1], Botao Song[1] and Quan Sun[1]

[1]Shanghai Electromechanical Engineering Institute, Shanghai, China

ABSTRACT.

Dense false target jamming has highly deceptive and suppressive characteristics, which may exist seriously impact on radar systems. Hence, based on the principle that jammers generate dense false target jamming, a waveform design method of dense false target jamming suppression is proposed to solve this problem. A criterion to design deceptive pulse and radar effective waveform is proposed through minimizing cross correlation level of dense false target jamming and radar effective waveform, and autocorrelation sidelobe level of radar effective waveform. The criterion could be solved by the least-pth algorithm. Simulation results indicate that the radar waveform designed by the proposed method could effectively suppress the dense false target jamming.

Keywords: dense false target jamming, deceptive waveform, waveform design, peak sidelobe level, phase coded waveform

1. INTRODUCTION

With the rapid development of high-speed integrated circuit technology and digital signal processing technology, digital radio frequency memory [1] (DRFM) technology and direct digital synthesis technology make interference technologies of modern radar gradual agility, diversity and intelligence. Jammers based on DRFM technology store the sampled radar signals, modulate some parameters of the stored signals and then release them at the appropriate time. The dense false target signals generated by jammers could simulate some characteristics of typical targets [2]. This kind of false target signal has strong deceptive and suppressive characteristics, resulting in dense false target signals that may be mistaken for real targets and the radar system has no other resources to search or track real targets. Therefore, it is one of the difficulties to suppress dense false target jamming in the current radar field [2-4].

There are lots of methods to suppress the dense false target jamming. In [5], a bi-phase random coded waveform is proposed to reduce the correlation among coherent processing intervals. Due to the mismatch with referenced waveform, the dense false target jamming could be suppressed. In [6], the correlation coefficient between the signal in the main channel and that in the auxiliary channel is firstly calculated and then adaptive sidelobe canceller is utilized to eliminate the jamming signals. A method based on enhanced three-dimensional joint domain localized space time adaptive processing is proposed in [7] to suppress the dense false target jamming. But this method is only applied to frequency diverse array multi-input multi-output radar and has high complexity. In [8], based on the differences in the frequency response characteristics of the radar and DRFM jammer, a method of a fast-slow time domain joint frequency response feature is utilized to counter dense false target jamming. [9] uses minimum variance distortionless response spatial domain filtering to filter out the dense false target jamming from the azimuth of jammer. It is worth noting that the methods mentioned above are mainly suppressed the dense false target jamming at the radar receiver end and not actively countered at the radar transmitter.

Therefore, in order to suppress dense false target jamming, based on the principle that jammers produce dense false target jamming, this paper proposes a waveform design criterion to design deceptive pulses and radar effective transmitting signal. The design criterion is to minimize the cross correlation level of the dense false target jamming and radar effective transmitting signal, and the autocorrelation sidelobe level of radar effective transmitting signal, which is a non-convex optimization problem. In this paper, a least-*p*th minimax algorithm [10] is utilized to solve this problem.

[1] [a] 1765283243@qq.com

The International Conference Optoelectronic Information and Optical Engineering (OIOE2024), edited by Yang Yue, Lu Leng, Proc. of SPIE Vol. 13513, 135131Z · © 2025 SPIE · 0277-786X · © The Authors. Published under a Creative Commons Attribution CC-BY 3.0 License · doi: 10.1117/12.3045611

Numerical simulation results show that the radar waveform designed by the proposed method could effectively suppress dense false target jamming.

2. SIGNAL MODEL

In order to protect real targets, the jammer needs to detect radar transmitting signal as far as possible. Hence, the receiver of jammer usually needs a relatively high sensitivity. In addition, in order to ensure a high correlation between the interference signal generated by jammer and radar signal sampled by jammer, the time delay between the interference signal and radar signal needs to be small as soon as possible. Therefore, the jammer usually adopts the mode of transmitting and receiving at the same time. However, in engineering practice, it is difficult to simultaneously meet the requirements of high receiving sensitivity and high transceiver isolation for the jammer. Therefore, the jammer usually adopts a time-sharing mode of transmitting and receiving.

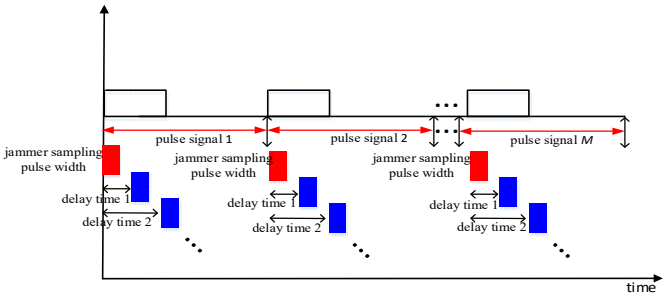

Figure. 1 The same period of false target period and radar pulse period

In the time-sharing working mode of transmitting and receiving, in order to ensure that the generated interference signal has a high correlation with the radar current pulse signal, the jammer usually chooses to sample the rising edge of pulse signal and modulates different parameters such as time delay, velocity and so on (see figure 1). It should be noted that (1) the sampling pulse width of the jammer is related to the radar signal pulse width, the distance of the false target closest to the real target and other factors. (2) In order to protect real target, the false target distance is closely related to that of the real target and the distance interval of false target and real target gradually increases. (3) The jammer of sampling radar pulse is a trigger type, in other words when there exists a radar signal, it samples and generates false target signals.

If the sum of time delay of the false target farthest from the real target and the duration time of the jammer sampling radar signal is larger than the pulse width of radar signal, as shown in figure 1, the period of false target is the same as that of radar signal period. Otherwise, as shown in figure 2 , then the period of false target is smaller than that of radar pulse period.

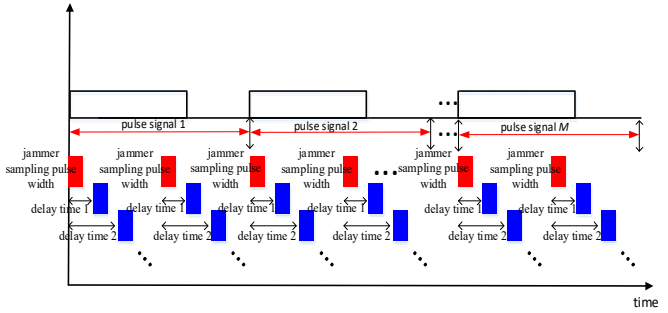

Figure. 2 The different periods of false target period and radar pulse period

The radar transmitting signal can be expressed as $s(t) = A \cdot exp(j\,2\,\pi f_0\,t + j\,\phi\,(t))$, where f_0 is the signal carrier frequency, $\phi(t)$ is the signal phase and A is the signal amplitude. Assume that the jammer samples the width of radar signal T_{val} and the time interval between adjacent false targets is T_J, then the signal expression of the jammer sampling radar signal and generating dense false target jamming can be expressed by

$$J(t) = \text{rect}\left(\frac{t}{T_{\text{val}}}\right) s(t) \otimes \sum_{m=1}^{K} A_J \cdot \delta\left(t - \tau - (m-1) * T_J\right) \tag{1}$$

where m is the index of the mth false target time delay, τ is time delay of the first false target, $\otimes$ represents convolution operation, A_J is the amplitude of interference signal modulated by the jammer, and $\delta(\cdot)$ is the impact function. The false target signal after matching filter can be expressed as

$$r(t) = J(t) \otimes s^*(-t) \tag{2}$$

where $(\cdot)^*$ is the conjugate operation.

Combining of equation (1) and equation (2), it can be seen that the interference signal and radar signal have a certain relevant, which is proportional to the width T_{val}.

Assume that the ith radar pulse signal after mixing sampling can be expressed as $\boldsymbol{s}_i \in \mathbb{C}^{N_s \times 1}$, then the signal $\boldsymbol{s}_i$ after matching filter could be written as

$$\rho_{i,k} = \frac{\boldsymbol{s}_i^H \boldsymbol{J}_k \boldsymbol{s}_i}{N_s} \tag{3}$$

where $i = 1,2,\cdots,M$, M is the total number of signals transmitted by the radar within one frame, $\rho_{i,k}$ indicates the match filter result of the kth range bin. When k is 0, $\rho_{i,0}$ denotes the mainlobe after matching filter, and conversely, $\rho_{i,k}$ is the sidelobe level after matching filter, $(\cdot)^H$ represents the conjugate transpose operation, $\boldsymbol{J}_k$ is a shift matrix, the expression [11] is

$$\boldsymbol{J}_k = \boldsymbol{J}_{-k}^T = \begin{bmatrix} \boldsymbol{0}_{(N_s-k)\times k} & \boldsymbol{I}_{N_s-k} \\ \boldsymbol{0}_{k\times k} & \boldsymbol{0}_{k\times(N_s-k)} \end{bmatrix}, 0 \le k \le N_s \tag{4}$$

where $(\cdot)^T$ is the transpose operation, $\boldsymbol{0}$ is the all-zero matrix, $\boldsymbol{I}$ represents the identity matrix. The sidelobe levels of signal after matching filter $\rho_{i,k}$ satisfy

$$\rho_{i,-k} = \frac{\boldsymbol{s}_i^H \boldsymbol{J}_{-k} \boldsymbol{s}_i}{N_s} = \frac{\left(\boldsymbol{s}_i^H \boldsymbol{J}_k \boldsymbol{s}_i\right)^H}{N_s} = \rho_{i,k}^* \tag{5}$$

It can be seen from the above formula that $\left|\rho_{i,k}\right| = \left|\rho_{i,-k}\right|$, namely, the amplitude of sidelobe level is symmetric about $\rho_{i,0}$, where $|\cdot|$ is the module value operation. For ease of expression, let $\boldsymbol{\rho}_{i,side}$ be the sidelobe level vector of signal $\boldsymbol{s}_i$ after matching filter, that is

$$\boldsymbol{\rho}_{i,\text{side}} = \left[\rho_{i,1}, \rho_{i,2}, \cdots, \rho_{i,N_s-1}\right]^T \tag{6}$$

Combine all sidelobe levels into a vector, namely,

$$\boldsymbol{\rho}_{\text{side}} = \left[\boldsymbol{\rho}_{1,\text{side}}^T, \boldsymbol{\rho}_{2,\text{side}}^T, \cdots, \boldsymbol{\rho}_{M,\text{side}}^T\right]^T \tag{7}$$

In order to reduce the impact of false target signals on the radar, the radar could use some methods such as frequency agility to deceive jammers in the frequency domain. However, the available frequency band resources for radar are limited, especially for low-frequency radar, which is difficult to simultaneously satisfy the characteristics of large instantaneous bandwidth and arbitrary frequency agility. Therefore, we can design phase coded waveform to trick the jammer in the time domain. Combining Fig. 1 and Fig. 2, it can be seen that the jammer usually samples the rising edge or other parts of the pulse width (when the radar pulse width is relatively large, the jammer may collect multiple parts of the same pulse). Therefore, in order to improve the detection performance of radar, the phase coded waveform design needs to consider the following three aspects. Firstly, a deceptive phase coded waveform in front of the real radar pulse signal could be considered, as shown in Figure 3, whose cross correlation level after matching filter needs to be as low as possible. Secondly, the jammer samples partial effective pulse width of the real radar transmitting signal, and the cross correlation level after matching filter is also as low as possible. Thirdly, the autocorrelation sidelobe level of the real radar signal after matching filter needs to be as low as possible.

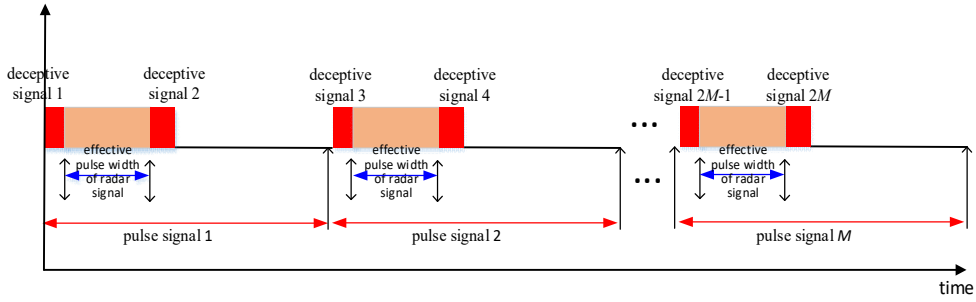

Figure. 3 Schematic diagram of deceptive pulse signal

Assume that the deceptive pulse signal is $\boldsymbol{Z} = [\boldsymbol{z}_1, \boldsymbol{z}_2, \cdots, \boldsymbol{z}_{2M}]$, the expression at the range bin k of deceptive pulse signal $\boldsymbol{z}_i$ after matching filter could be written as

$$\omega_i(k) = \begin{cases} \sum_{n=-\infty}^{\infty} \boldsymbol{z}_i(n)\, \boldsymbol{s}^*_{\frac{(i+1)}{2}}(n-k), & i \text{ is odd} \\ \sum_{n=-\infty}^{\infty} \boldsymbol{z}_i(n)\, \boldsymbol{s}^*_{\frac{i}{2}}(n-k), & i \text{ is even} \end{cases} \tag{8}$$

where $i = 1,2,\cdots,2M$. The nth element of the deceptive pulse signal can be expressed as

$$\boldsymbol{z}_i(n) = \begin{cases} e^{j\boldsymbol{\varphi}_i(n)}, n \in [1, N_J] \\ 0, \text{others} \end{cases} \tag{9}$$

where $\boldsymbol{\varphi}_i$ is the phase vector of deceptive pulse signal. Let $\boldsymbol{\omega}_i$ be the cross correlation level vector of the deceptive pulse $\boldsymbol{z}_i$ after radar matching filter. The specific expression is

$$\boldsymbol{\omega}_i = \left[\omega_i\left(1 - \frac{(N_s+N_J)}{2}\right), \omega_i\left(2 - \frac{(N_s+N_J)}{2}\right), \cdots, \omega_i\left(\frac{(N_s+N_J)}{2} - 1\right)\right]^T \tag{10}$$

In order to form a vector, arrange the cross correlation levels $\boldsymbol{\omega}_i$（$\forall i$）of all deceptive pulses, as shown below

$$\boldsymbol{\omega}_{\text{cross}} = [\boldsymbol{\omega}_1^T, \boldsymbol{\omega}_2^T, \cdots, \boldsymbol{\omega}_{2M}^T]^T \tag{11}$$

If the sampling location of jammer is the position where the radar actually transmits effective pulse signals (for simplicity, referred as jammer sampling pulse), the sampling pulse signals within one frame can be expressed as $\boldsymbol{R} = [\boldsymbol{r}_1, \boldsymbol{r}_2, \cdots, \boldsymbol{r}_q]^T$, where q is the total number of jammer sampling radar effective pulses. The expression of jammer sampling pulse $\boldsymbol{r}_m$ at range bin k is expressed as

$$\gamma_m(k) = \sum_{i=1}^{N_t} \sum_{n=-\infty}^{\infty} \boldsymbol{r}_m(n)\, \boldsymbol{s}_i^*(n-k) \tag{12}$$

where $m = 1,2,\cdots,q$. The nth element of the sampling pulse can be expressed as

$$\boldsymbol{r}_m(n) = \begin{cases} e^{j\boldsymbol{\theta}_m(n)}, n \in [1, N_J] \\ 0, \text{others} \end{cases} \tag{13}$$

where $\boldsymbol{\theta}_m$ is the phase vector of the jammer sampling pulse $\boldsymbol{r}_m$. Let $\boldsymbol{\gamma}_m$ be the cross correlation level vector of the sampling pulse $\boldsymbol{r}_m$ after radar matching filter. The specific expression is

$$\boldsymbol{\gamma}_m = \left[\gamma_m\left(1 - \frac{(N_s+N_J)}{2}\right), \gamma_m\left(2 - \frac{(N_s+N_J)}{2}\right), \cdots, \gamma_m\left(\frac{(N_s+N_J)}{2} - 1\right)\right]^T \tag{14}$$

In order to form a vector, arrange the cross correlation levels $\boldsymbol{\omega}_i$ （$\forall i$） of all sampling pulses, as shown below

$$\boldsymbol{\gamma}_{\text{cross}} = [\boldsymbol{\gamma}_1^T, \boldsymbol{\gamma}_2^T, \cdots, \boldsymbol{\gamma}_q^T]^T \tag{15}$$

3. DESIGN CRITERIA

Under strong targets, multiple targets, strong clutter or multiple clutter environments, high range sidelobes can easily trigger false alarms or submerge weak targets causing missed alarms. Therefore, in order to improve radar detection performance, one of the waveform design criteria is to reduce the autocorrelation sidelobe level and the cross correlation level among different signals after radar matching filter [12].

In order to better suppress dense false target jamming, waveform design criteria need to consider the following two aspects:

(1) Suppress autocorrelation sidelobe level: waveform design by suppressing the integrated sidelobe level may cause high sidelobe levels of some range bins. In order to improve the detection performance of weak and small targets, it is proposed to minimize the autocorrelation peak sidelobe level (APSL), i.e.

$$\min_{\boldsymbol{\psi}} max|\boldsymbol{\rho}_{\text{side}}| \tag{16}$$

where $\boldsymbol{\psi}$ is the phase of signal $\boldsymbol{S} = [\boldsymbol{s}_1, \boldsymbol{s}_2, \cdots, \boldsymbol{s}_M]$, namely, $\boldsymbol{S} = exp(j\boldsymbol{\psi})$. The formula above can be simplified to

$$\min_{\boldsymbol{\psi}} \|\boldsymbol{\rho}_{\text{side}}\|_\infty \tag{17}$$

where $\|\cdot\|_\infty$ is the infinite norm.

(2) Suppress cross correlation level: in order to suppress dense false target jamming, a design criterion of minimizing peak cross correlation level (PCCL) is proposed

$$\min_{\boldsymbol{\varphi},\boldsymbol{\theta}} max|\boldsymbol{\omega}_{\text{cross}}| + max|\boldsymbol{\gamma}_{\text{cross}}| \tag{18}$$

where $\boldsymbol{\varphi}$ is the phase vector of deceptive pulse $\boldsymbol{Z}$, and $\boldsymbol{\theta}$ is the phase vector of jammer sampling pulse $\boldsymbol{R}$. Since the sampling pulse is the part of radar effective pulse signal, the phase of the sampling signal is part phase of the real radar signal, namely $\boldsymbol{\theta} \in \boldsymbol{\psi}$. The formula above can be simplified to

$$\min_{\boldsymbol{\varphi},\boldsymbol{\theta}} \|\boldsymbol{\omega}_{\text{cross}}\|_\infty + \|\boldsymbol{\gamma}_{\text{cross}}\|_\infty \tag{19}$$

Comprehensive the design criteria of equation (17) and equation (19), the design criteria of suppressing dense false target jamming can be expressed as

$$\min_{\boldsymbol{\psi},\boldsymbol{\varphi},\boldsymbol{\theta}} \|\boldsymbol{\rho}_{\text{side}}\|_\infty + \alpha_1\|\boldsymbol{\omega}_{\text{cross}}\|_\infty + \alpha_2\|\boldsymbol{\gamma}_{\text{cross}}\|_\infty \tag{20}$$

where α_1 and α_2 are the weight coefficients of cross correlation level. The values of α_1 and $\alpha_2$need to be preset manually to weigh the performance of APSL and PCCL. Based on practical engineering requirements, the parameters could be manually adjusted to obtain the desired results when optimizing the objective function.

4. OPTIMIZATION ALGORITHM

The objective function in the equation (20) is non-smooth and the conventional optimization algorithm requires taking derivatives of the objective function, so the objective function needs to be transformed. According to the properties of the norm, we can obtain

$$\lim_{p\to\infty}\|\boldsymbol{\rho}_{\text{side}}\|_p = \|\boldsymbol{\rho}_{\text{side}}\|_\infty \tag{21}$$

where $\|\cdot\|_p$ represents the *p*-norm. In order to minimize $\|\boldsymbol{\rho}_{\text{side}}\|_\infty$, we can gradually increase the value p [10] to gradually minimize $\|\boldsymbol{\rho}_{\text{side}}\|_p$, thus it is approximately equal to minimizing $\|\boldsymbol{\rho}_{\text{side}}\|_\infty$. Similarly, it can be seen that minimizing $\|\boldsymbol{\omega}_{\text{cross}}\|_\infty$ and $\|\boldsymbol{\gamma}_{\text{cross}}\|_\infty$ could be approximated by gradually minimizing $\|\boldsymbol{\omega}_{\text{cross}}\|_p$ and $\|\boldsymbol{\gamma}_{\text{cross}}\|_p$. Define a function

$$f(\boldsymbol{x}) = \|\boldsymbol{\rho}_{\text{side}}\|_p + \alpha_1\|\boldsymbol{\omega}_{\text{cross}}\|_p + \alpha_2\|\boldsymbol{\gamma}_{\text{cross}}\|_p \tag{22}$$

where the vector $\boldsymbol{x}$ is a column vector composed of $\boldsymbol{\psi}, \boldsymbol{\varphi}, \boldsymbol{\theta}$ in order.

The detailed steps of the iterative suppression algorithm based on *p*-norm are as follows:

(1) Set initial value $\boldsymbol{x}_0$ of the objective function and the threshold ε_1 of the minimum value of the two adjacent iterations, and let the parameters $i = 1,\ p = 2,\ \mu = 2,\ f_0 = 10000$;

(2) Set vector $\boldsymbol{x}_{i-1}$ be the initial value of the *i*th iteration, and the optimization result $\boldsymbol{x}_i$ of this time can be obtained through suppressing $f(\boldsymbol{x})$, and let $f_i = f(\boldsymbol{x}_i)$;

(3) If $|f_{i-1} - f_i| < \varepsilon_1$, obtain the final optimization result $\boldsymbol{x}_i$ and stop optimization. Otherwise, set $p = \mu p,\ i = i + 1$, return to step (2).

Due to the constraint of radar waveform constant modulus, the function $f(\boldsymbol{x})$ in step (2) is a non-convex function. We can use Newton algorithm or quasi-Newton algorithm to optimize the objective function. Compared with the Newton algorithm, the quasi-Newton algorithm could reduce the computational complexity by approximating the Hessian matrix. Since the computational complexity of the quasi-Newton algorithm is proportional to the square of function dimension, this algorithm still requires extensive computation when the objective function dimension is high. Hence, this paper uses the L-BFGS algorithm [13] to minimize the function $f(\boldsymbol{x})$. This algorithm could construct the Hessian matrix based on few vectors, which not only reduces the amount of computation, but also could be easier to implement. The specific process of the algorithm is as follows:

Parameter initialization: set the number of updates m, the starting value of the iteration index $i = 0$, the initial value of the variable $\boldsymbol{x}_0$ and calculate the function f_0 and the first-order partial derivatives of the function ∇f_0, let the search direction of the objective function be $\boldsymbol{g}_0 = -\nabla f_0$. Algorithm iteration steps as follows,

(1) Obtain λ_i using line search method based on f_i, ∇f_i and $\boldsymbol{g}_i$;

(2) Calculate $\boldsymbol{z}_i = \lambda_i \boldsymbol{g}_i$, $\boldsymbol{x}_{i+1} = \boldsymbol{x}_i + \lambda_i \boldsymbol{g}_i$;

(3) Calculate ∇f_{i+1} and $\boldsymbol{y}_i = \nabla f_{i+1} - \nabla f_i$;

(4) Let $\boldsymbol{q} = \nabla f_{i+1}$;

(5) for $n = i, i-1, \cdots, i-m+1$

$$t_n = \frac{\boldsymbol{z}_n^H \boldsymbol{q}}{\boldsymbol{y}_n^H \boldsymbol{z}_n}, \boldsymbol{q} = \boldsymbol{q} - t_n \boldsymbol{y}_n$$

end

(6) $\boldsymbol{r} = \frac{\boldsymbol{z}_n^H \boldsymbol{y}_n}{\boldsymbol{y}_n^H \boldsymbol{y}_n} \boldsymbol{q}$;

(7) for $n = i-m+1, i-m+2, \cdots, i$

$$\beta = \frac{\boldsymbol{y}_n^H \boldsymbol{r}}{\boldsymbol{y}_n^H \boldsymbol{x}_n}, \boldsymbol{r} = \boldsymbol{r} + (t_n - \beta)\boldsymbol{z}_n$$

end

(8) $\boldsymbol{g}_{i+1} = -\boldsymbol{r}$;

(9) $i = i + 1$;

until the set termination condition is reached.

Steps (5) to (8) of the iteration process above are mainly based on the first-order partial derivative information of adjacent m times to approximate the product of the Hessian matrix and $\boldsymbol{q}$ (namely, vector $\boldsymbol{r}$), which iterate m times based on vector $\boldsymbol{r}$ to obtain search direction of the next iteration. The computation amount of this algorithm mainly comes from solving the objective function $f(\boldsymbol{x})$ and $\nabla f(\boldsymbol{x})$. Without loss of generality, the computation amount only counts the number of complex multiplications. It needs require $O\left(M^2\left(N_s + N_J\right)\left(log_2\left(N_s + N_J\right) + p\right) + pMN_J\right)$and $O\left(pM^2\left(N_s + N_J\right)\right)$ times of complex multiplications, respectively, to solve functions $f(\boldsymbol{x})$ and $\nabla f(\boldsymbol{x})$.

5. SIMULATION RESULTS

In this section, the feasibility of the proposed algorithm above is verified by simulations. Assume that the length of phase coded waveform is $N_s = 256$, and the subcode width of transmit pulse is 1us. Since the jammer based on DRFM usually quantizes the phase of sampling signal, and then modulates information such as time delay, velocity and amplitude, modulation mechanism is irrelevant to the parameters of real radar transmit signal. Therefore, without loss of generality, the parameters of radar effective pulse signal within one frame are same and the parameters of radar deceptive pulse within one frame are also same. Next, the effects of suppressing false targets are analyzed at different distances from the minimum starting distance of the false target relative to that of the real target.

Unless otherwise specified, the distance mentioned below specifically refers to the minimum starting distance of the false target relative to that of the real target (short for the starting distance), and the weight coefficients $\alpha_1 = 1$ and $\alpha_2 = 1$ in equation (20). Assume that the jammer sampling pulse width is 2us~32us, and the specific suppression effects

of false targets are shown in the different simulation experiments below. Since the objective function in equation (20) is non-convex, different initial values may lead to different optimization results. Therefore, the each simulation experiment below generates 30 groups of initial values for optimization and the optimization results with the smallest objective function value are selected as the final results.

5.1 Influence analysis of starting distance

5.1.1 Starting distance is 45km

When the starting distance is 45km, the minimum time interval of jammer to start the next sampling is about 300us. Since the maximum of total width of radar effective pulse and deceptive pulse is 288us, the jammer only samples one sample during each radar transmit pulse signal. In other words, the sampling signal of jammer is a deceptive pulse.

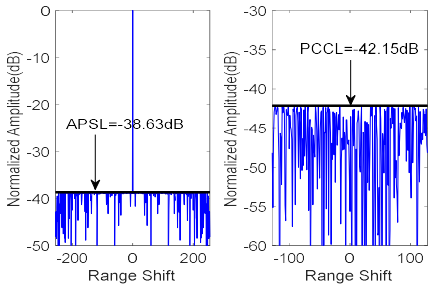

Figure.4 Sampling length of jammer is 2us

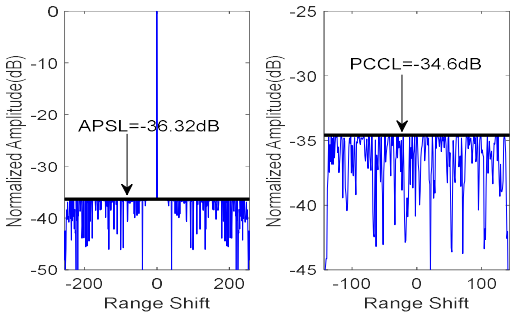

Figure.5 Sampling length of jammer is 32us

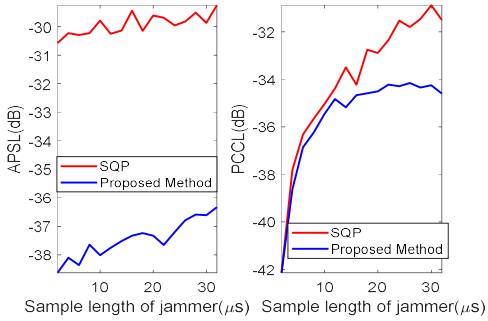

Figure.6 APSL and PCCL vary with sampling length

From Fig.4 to Fig.6, we can see that as the sampling length of jammer (i.e., the deceptive pulse length) increases, APSL and PCCL gradually increase. This is mainly because the degrees of freedom of radar effective pulse signal are fixed, with sampling length increasing, more degrees of freedom are used to suppress the deceptive pulse and thus the degree of freedom of suppressing the autocorrelation sidelobe levels of radar pulse signal is reduced, resulting in the increasing of sidelobe levels. Fig.6 compares the results of the proposed method and the sequential quadratic programming (SQP) method. It can be seen that the optimization method in this paper could achieve lower sidelobe level. In addition, from Fig.6, we can see that as the sampling length of jammer increases, the APSL and PCCL show small fluctuations. This is

mainly because the objective function of equation (20) is non-convex, and different initial values may lead to different results.

5.1.2 Starting distance is 20km

When the starting distance is 20km, the minimum time interval of jammer to start the next sampling is about 133.33us. Since the maximum of total width of radar effective pulse and deceptive pulse is 258us~288us, the samples of jammer are sampled twice during each radar transmit pulse signal. In other words, one of the sampling signal is a deceptive pulse, the other is the radar effective pulse signal.

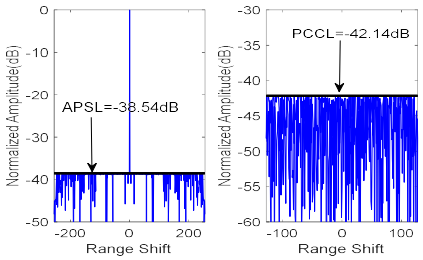

Figure.7 Sampling length of jammer is 2us

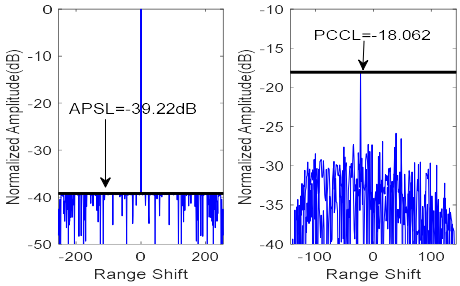

Figure.8 Sampling length of jammer is 32us

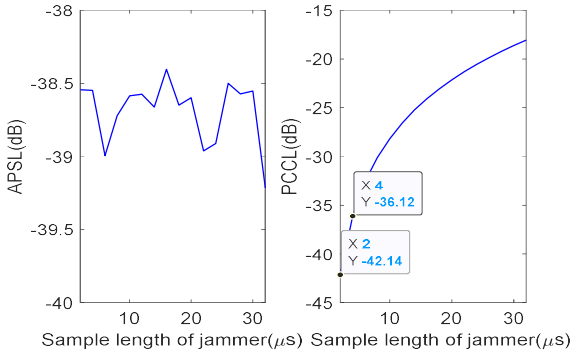

Figure.9 APSL and PCCL vary with sampling length

From Fig.7 to Fig.9, it can be seen that as the sampling length of jammer increases, PCCL gradually increases and APSL maintains small range fluctuations. This is mainly due to the weight coefficient $\alpha_1 = \alpha_2 = 1$ of equation (20). When the sampling length is large (≥4us), PCCL is higher than APSL, the optimization algorithm are mainly used to minimize PCCL. In addition, comparing Fig.7 with Fig.8, it can be seen that there is a large peak in Fig.8. This is because the jammer samples part of the radar effective pulse width, and the longer the sampling length is, the higher the correlation with the radar effective pulse signal is, which results in a higher PCCL.

5.1.3 Starting distance is 10km

When the starting distance is 10km, the minimum time interval of jammer to start the next sampling is about 66.67us. Since the maximum of total width of radar effective pulse and deceptive pulse is 288us, the samples of jammer are

sampled four times during each radar transmit effective pulse signal. In other words, one of the sampling signal is a deceptive pulse, the others are the radar effective pulse signals.

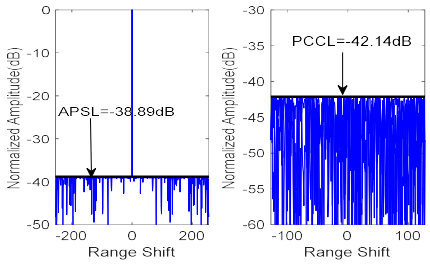

Figure.10 Sampling length of jammer is 2us

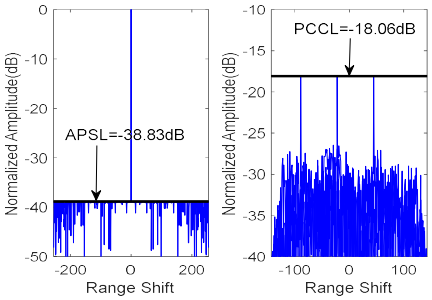

Figure.11 Sampling length of jammer is 32us

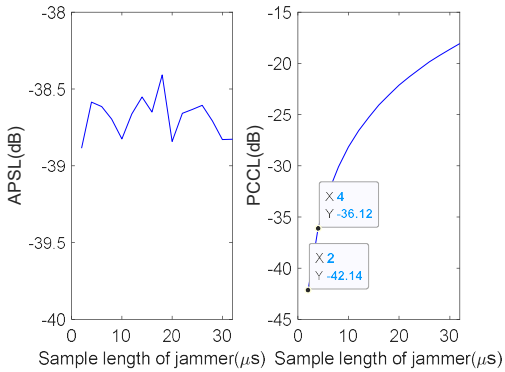

Figure.12 APSL and PCCL vary with sampling length

Similarity, from Fig.10 to Fig.12, it can be seen that as the sampling length of jammer increases, PCCL gradually increases, and APSL remains small range fluctuations. Comparing Fig.11 with Fig.8, it can be seen that there are three peaks in Fig.11. This is mainly because the jammer is trigger type and if the starting distance of false target is small, the time interval of two adjacent sampling by the jammer becomes small. Under the condition that the radar effective pulse width is fixed, the smaller the time interval is, the more times the radar effective pulse width may be sampled, which results in more cross correlation peak values.

5.2 Influence analysis of radar pulse width

Under the condition that the jammer sampling length is fixed ($N_J = 16$), analyze the influence of different radar pulse widths (namely, the length of phase coded waveform N_s) on the results of waveform design.

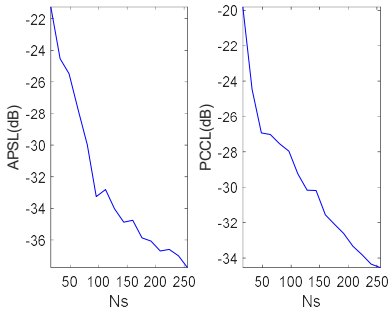

Figure.13(a) starting distance is 45km

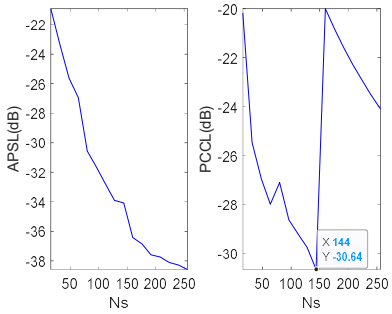

Figure.13(b) starting distance is 20km

Figure.13 APSL and PCCL vary with radar pulse width

It can be seen from Fig.13(a) that as the length of phase coded waveform increases, APSL and PCCL gradually decrease. This is mainly because the samples sampled by the jammer are deceptive pulse signals under the condition that the starting distance is 45km. The length of phase coded waveform increases, which means increasing the degree of freedom of optimization algorithm, and more degrees of freedom could obtain better results.

In addition, from Fig.13(b), we can see that as the length of phase coded waveform increases, APSL gradually decreases and PCCL first gradually decreases, then jumps and final gradually decreases. This is mainly because the starting distance is 20km, with the code length increasing, the sampling signal of the jammer changes from the only deceptive pulse to the deceptive pulse and the partial radar effective pulse, which results in the phenomenon of PCCL transition. In addition, since the effective pulse sampled by the jammer is fixed, as the code length increases, the cross correlation of the sample and the radar pulse signal gradually decreases, so the PCCL gradually decreases after the transition.

Based on Fig.13(a) and Fig.13(b), in order to reduce the influence of dense false target jamming, it could be considered to appropriately reduce the effective width of radar pulse signal. Since the SNR of target echo is proportional to the total energy radiated by radar, in practice, the SNR of target could be ensured by reducing the effective width of a single pulse and increasing the number of pulses within one frame.

5.3 Influence analysis of weight coefficient

The cross correlation levels are affected by the weight coefficients α_1 and α_2 in equation (20). In order to facilitate the analysis of the weight coefficient effects on APSL and PCCL, without loss of generality, let the weight coefficient $\alpha = \alpha_1 = \alpha_2$.

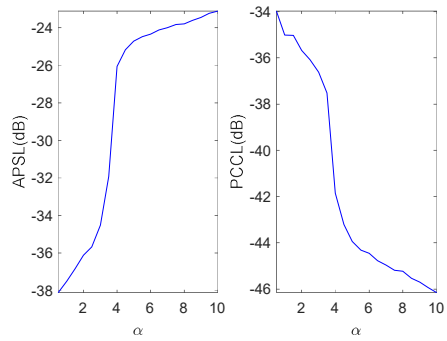

Figure.14 APSL and PCCL vary with weight coefficients

From Fig.14, we can see that as the coefficient α increases, APSL gradually increases and PCCL gradually decreases. This is mainly because increasing α is equivalent to increasing the weight coefficient of PCCL (equivalent to decreasing the weight coefficient of APSL), hence the PCCL gradually decreases and the APSL gradually increases. In practice, we could choose appropriate weight coefficients based on different application scenarios.

5.4 Influence analysis of Doppler frequency mismatch

Without loss of generality, the phase coded waveforms optimized are randomly selected to analyze Doppler frequency effects.

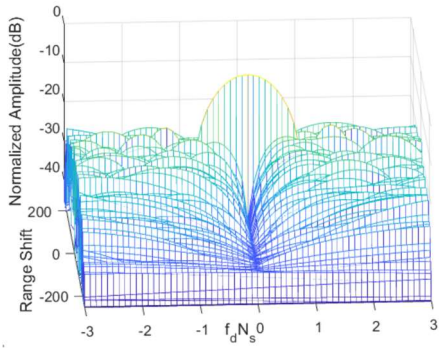

Figure.15 Ambiguity function of phase coded waveform

It should be noted that f_d in Fig.15 is the Doppler frequency. From Fig.15, it can be seen that in the zero Doppler channel, the peak value is high and the sidelobe level is much low. But Doppler frequency increases (namely, Doppler mismatch), the peak value of target decreases and the sidelobe level first gradually increases and then fluctuates irregularly. In practical applications, if the radar is in search mode and the velocity of target is unknown, the radar at the receiving end could use some match filters modulating different Doppler frequencies to match filter. If the radar is in tracking mode and the velocity of target is known, the match filter at the radar receiving end modulated the Doppler frequency could be used to filter the echoes of targets.

6. CONCLUSION

In this paper, a method of phase coded waveform design is proposed to suppress false targets based on the principle that jammers produce dense false target jamming. The criteria is to minimize the PCCL of the false target signal and the radar effective signal, and to simultaneously minimize the APSL of the radar effective signal, which could be solved through the least-*p*th algorithm using the L-BFGS algorithm as its sub-algorithm. Simulation results show that the phase coded waveform by the proposed method can effectively suppress dense false target jamming. However, when the effective pulse width of radar is wide, the jammer may sample the radar effective pulse signal, which causes the PCCL to rise. In addition, the influences of different parameters on the optimization results are analyzed, providing a theoretical basis for subsequent engineering applications.

7. REFERENCES

[1] Berger Scott D. Digital radio frequency memory linear range gate stealer spectrum. IEEE Transactions on Aerospace and Electronic Systems, 2003, 39(2): 725-735.

[2] Poisel Richard A. Information Warfare and Electronic Warfare Systems. Boston: Artwch House, 2013.

[3] Graham Adrian. Communications radar and electronic warfare. New York: Wiley, 2011.

[4] Li Nengjing. Zhang Yiting. A survey of radar ECM and ECCM. IEEE Transactions on Aerospace and Electronic Systems, 1995, 31(3): 1110-1120.

[5] Wang Baozhi, Yang Xiaopeng, Yang Zhongwei, et al. Dense false-target jamming suppression method by utilizing bi-phase random coded waveform for space time adaptive processing. IET International Radar Conference, 2020, 1531-1534.

[6] Cai Guang, Shao Yinbo, Li Rongfeng, et al. A method for countering dense false target jamming based on correlation sample selection. IEEE International Conference on Signal Processing, Communications and Computing, 2017, 1-5.

[7] Wen Cai, Peng Jinye, Zhou Yan, et al. Enhanced Three-Dimensional joint Domain Localized STAP for Airborne FDA-MIMO Radar Under Dense False-Target Jamming Scenario, IEEE Sensors Journal, 2018, 18(10): 4154-4166.

[8] Peng Ruihui, Wei Wenbin, Sun Dianxing, et al. Dense False Target Jamming Recognition Based on Fast-Slow Time Domain Joint Frequency Response Features. IEEE Transactions on Aerospace and Electronic Systems, 2023, 59(6): 9142-9159.

[9] Yin Xianhan, Fu Xiongjun, Xie Min, et al. Range-Angle Two-Dimensional Anti-jamming Against Dense False Targets. IET International Radar Conference, 2020, 165-170.

[10] Antoniou Andreas, Lu Wusheng. Practical optimization: algorithm and engineering application. Springer, 2007.

[11] Song Xiufeng, Zhou Shengli, Willett Peter. Reducing the waveform cross correlation of MIMO radar with space–time coding. IEEE Transactions on Signal Processing, 2010, 58(8): 4213-4224.

[12] Akbaripour Amirmokhtar, Bastani Mohammad H. Range sidelobe reduction filter design for binary coded pulse compression system. IEEE Transactions on Aerospace and Electronic Systems, 2012, 48(1): 348-359.

[13] Wang Yongchao, Wang Xu, Liu Hongwei, et al. On the design of constant modulus probing signals for MIMO radar. IEEE Transactions on Signal Processing, 2012, 60(8): 4432-4438.